Viscous and gravitational contributions to mixing during vertical brine transport in water-saturated porous media

Tracey C. Flowers[1,2] and James R. Hunt[1]

Received 6 December 2005; revised 28 May 2006; accepted 30 August 2006; published 10 January 2007.

[1] The transport of fluids miscible with water arises in groundwater contamination and during remediation of the subsurface environment. For concentrated salt solutions, i.e., brines, the increased density and viscosity determine mixing processes between these fluids and ambient groundwater. Under downward flow conditions, gravitational and viscous forces work against each other to determine the interfacial mixing processes. Historically, mixing has been modeled as a dispersive process, as viscous fingering, and as a combination of both using approaches that were both analytical and numerical. A compilation of previously reported experimental data on vertical miscible displacements by fluids with significant density and viscosity contrasts reveals some agreement with a stability analysis presented by Hill (1952). Additional experimental data on one-dimensional dispersion during downward displacement of concentrated salt solutions by freshwater and freshwater displacement by brines support the stability analysis and provides an empirical representation for dispersion coefficients as functions of a gravity number and a mobility ratio.

Citation: Flowers, T. C., and J. R. Hunt (2007), Viscous and gravitational contributions to mixing during vertical brine transport in water-saturated porous media, *Water Resour. Res.*, *43*, W01407, doi:10.1029/2005WR004773.

1. Introduction

[2] It is well known that groundwater is impacted by dense fluids miscible with water. Seawater intrusion into coastal aquifers is a long-standing problem, and dense fluids dominate groundwater flow near salt domes and beneath leaking municipal landfills [*Frind*, 1982; *Oostrom et al.*, 1992; *Hassanizadeh and Leijnse*, 1995; *Zhang and Schwartz*, 1995; *Jiao and Hötzl*, 2004]. Predictive models for contaminant transport in natural aquifers have greatly benefited from natural gradient tracer experiments, but there is recognition that plume transport is altered by tracer solutions having density contrasts with the ambient groundwater [*Istok and Humphrey*, 1995; *Barth et al.*, 2001]. Miscible transport processes in fluid-saturated porous media have direct bearing on the movement and recovery of brines and in determining the fate of contaminants present within brines. With the recognition that brine transport in the subsurface has increased relevance to contaminant migration and recovery, a synthesis of mechanisms, models, and data is appropriate. The need for additional experimental data justified an experimental component to this work.

[3] Industrial societies generate brines that impact groundwater resources, and Table 1 lists a few extreme examples. The oxidation of minerals produces acid rock drainage that is largely composed of sulfuric acid and can mobilize toxic metals. *Nordstrom et al.* [2000] investigated one of the most extreme cases at an abandoned mine where the solution has an approximate density of 1.4 g cm^{-3} estimated from a sulfate concentration of 760 g L^{-1}. The low pH and high ionic strength of mine drainage limits metal removal by adsorption and precipitation reactions and, as a consequence, trace metals concentrations are in the g L^{-1} range. For zinc and copper, the water quality standards listed in Table 1 are designed to protect aquatic life in surface waters, while the arsenic level is the recently revised drinking water standard. The final column of Table 1 is the volume of clean water required to dilute one volume of the waste solution to reach the water quality goal, and the ratio ranges from 10^4 to 10^5 for the species within this mine drainage water.

[4] Another example is landfill leachate, which is a complex mixture of dissolved organic and inorganic matter that can be denser than water. From a reported dissolved solids concentration of 45 g L^{-1} a fluid density of 1.03 g cm^{-3} is estimated. Leachates containing toxic chemicals such as vinyl chloride and degradable organic matter as represented by the 5-day biological oxygen demand (BOD_5) would require dilution factors of 10^4 to reach water quality objectives.

[5] Nuclear fuel reprocessing by the United States and the former Soviet Union produced brines saturated in $NaNO_3$ and contained very high levels of fission products [*Samsonova and Drozhko*, 1996]. The United States placed these brines in underground storage tanks that leaked and the former Soviet Union released its waste brines into a surface water reservoir that recharged a deep aquifer. To meet drinking water standards for the fission products ^{90}Sr and ^{137}Cs requires dilution factors of 10^{10} and 10^8, respectively, and even the nitrate level exceeds drinking water standard by 3 orders of magnitude.

[6] The final example of an industrial contaminant is ammonium perchlorate, NH_4ClO_4, which is a significant

[1]Department of Civil and Environmental Engineering, University of California, Berkeley, California, USA.
[2]Now at Exponent Inc., Menlo Park, California, USA.

0043-1397/07/2005WR004773$09.00

Table 1. Occurrence and Water Quality Impacts of Contaminated Brines

Occurrence	Source of Brine	Approximate Density, g cm^{-3}	Contaminant	Environmental Level	Water Quality Criteria	Dilution Required
Acid rock drainage	H_2SO_4	1.4	Zn	23.5 g L^{-1} [*Nordstrom et al.*, 2000]	100 μg L^{-1} [*U.S. Environmental Protection Agency (USEPA)*, 2000]	10^5
			Cu	4.8 g L^{-1} [*Nordstrom et al.*, 2000]	11 μg L^{-1} [*USEPA*, 2000]	10^5
			As	0.34 g L^{-1} [*Nordstrom et al.*, 2000]	10 μg L^{-1}[a]	10^4
Landfill leachate	dissolved solids	1.03	vinyl chloride	40 mg L^{-1} [*Gibbons et al.*, 1999]	2 μg L^{-1} [*American Water Works Association (AWWA)*, 1990]	10^4
			BOD_5	38 g L^{-1} [*Gettinby et al.*, 1996]	10 mg L^{-1}	10^4
Nuclear fuel processing	$NaNO_3$	1.5	^{90}Sr	4×10^{10} Bq L^{-1} [*Bell and Bell*, 1994]	10 Bq L^{-1} [*AWWA*, 1990]	10^{10}
			^{137}Cs	8×10^{9} Bq L^{-1} [*Bell and Bell*, 1994]	50 Bq L^{-1} [*AWWA*, 1990]	10^8
			NO_3^-	59 g L^{-1} [*Samsonova and Drozhko*, 1996]	45 mg L^{-1} [*AWWA*, 1990]	10^3
Solid rocket fuel	NH_4ClO_4	1.11	ClO_4^-	180 g L^{-1} [*Schumacher*, 1960]	6 μg L^{-1}[b]	10^7

[a]From http://www.epa.gov/safewater/arsenic.html accessed 24 October 2005.
[b]From http://www.dhs.ca.gov/ps/ddwem/chemicals/perchl/perchlindex.htm accessed 24 October 2005.

component of solid rocket fuel. The perchlorate anion is highly mobile in the subsurface since it is nonvolatile, does not engage in ion exchange reactions, and does not biodegrade under aerobic conditions [*Xu et al.*, 2003]. A saturated solution of ammonium perchlorate exceeds one proposed drinking water action level by at least 10^7.

[7] These examples of industrial wastes can be compared with coastal aquifers impacted by seawater intrusion, which only requires a hundredfold dilution to lower the dissolved solids concentration from 33 g L^{-1} to an acceptable level of 0.5 g L^{-1}. Table 1 suggests there are numerous contaminants present within brines where a small waste volume has the potential for contaminating large volumes of water. Mass transfer limitations on the recovery of these contaminants from concentrated brines in the subsurface were explored previously [*Flowers and Hunt*, 2000].

[8] Density and viscosity contrasts not only affect contaminant fate and transport processes, but also affect subsurface remediation technologies. These technologies can involve the injection of water-miscible fluids into the subsurface to accomplish contaminant destruction, isolation, and removal. Table 2 lists various remediation processes, the active compounds, their concentrations in the injected fluid, and the approximate fluid density and viscosity. Permanganate solutions are being injected into soils and aquifers for the destruction of organic matter, and the injected concentrations are high when the goal is the destruction of nonaqueous phase liquids. In situ bioremediation of halogenated solvents is promoted by methanogenic conditions achieved by injecting organic compounds such as sodium lactate at very high concentrations. One means of binding toxic metals to soil and aquifer materials is to add a concentrated liquid solution of calcium polysulfide, CaS_x, that decomposes and releases sulfide for trace metal precipitation as insoluble sulfides. Another approach to contaminant sequestration is to inject a colloidal silica suspension that gels and forms an impermeable barrier when mixed in situ with a concentrated NaCl solution. In addition, trapped nonaqueous phase organic liquids can be mobilized by the injection of alcohols for solubilization, or through the release of a denser brine from below to gravitationally mobilized the liquid.

[9] As Tables 1 and 2 indicate, there are many instances where brines and other concentrated solutions miscible with water are present in the subsurface environment or are planned for injection. These fluids have densities and viscosities distinct from ambient groundwater and these property differences can dominate their transport in the subsurface, the release of contaminants associated with brines into groundwater, or the delivery and recovery of remedial fluids. Quantitative models are needed to predict the transport of miscible fluids and guide in the implementation of remedial actions requiring the addition and mixing of reactive fluids. Following a macroscopic description of brine transport, mixing mechanisms are reviewed, experimental data from the literature are compared, and results from a new experimental program are presented that provide an empirical basis for predicting brine dispersion during vertical transport.

2. Conceptual Model

[10] Comparing Darcy's law for density driven brine migration and regional horizontal flow suggests that vertical

Table 2. Water-Miscible Fluids Injected for Subsurface Remediation

Purpose	Injected Fluid	Concentration	Density, g cm^{-3}	Viscosity, cP	References
Organics oxidation	$KMnO_4$	30 g L^{-1}	1.025	0.9	*Nelson et al.* [2001], *Lide* [2000]
Bioremediation	sodium lactate	60%	1.31	80–160	*Song et al.* [2002]
Metal binding	CaS_x	29%	1.27	17	*Yahikozawa et al.* [1978], *Aratani et al.* [1978a, 1978b], *Jacobs et al.* [2001]
Permeability reduction	colloidal silica	40% (w)	1.3	15	*Durmusoglu and Corapcioglu* [2000]
	NaCl (catalyst)	6% (w)	1.04	1.1	
NAPL mobilization	Tert-butyl alcohol	70%	0.867	5.42	*Roeder and Falta* [2001]
	Isopropal alcohol	60%	0.938	3.43	
NAPL mobilization	$CaBr_2$	56% (w)	1.75	6.65	*Johnson et al.* [2004]

flow dominates over horizontal flow for the brines encountered in Table 1. The vertical velocity of the brine in freshwater is estimated as

$$U_b = \frac{gk(\rho_b - \rho_w)}{n\mu_b} \tag{1}$$

where U_b is the vertical pore water velocity of the brine, k is the permeability of the aquifer, g is acceleration due to gravity, n is the porosity, μ_b is the viscosity of the brine, ρ_b is the brine density and ρ_w is the density of the ambient groundwater. For horizontal flow through porous media,

$$U_x = -\frac{\rho_w g k}{n\mu_w}\frac{dh}{dx} \tag{2}$$

where U_x is horizontal pore water velocity, μ_w is the kinematic viscosity of ambient groundwater and dh/dx is the hydraulic gradient. The ratio of the magnitudes of the vertical brine velocity to the horizontal velocity from equations (1) and (2) becomes

$$\frac{U_b}{U_x} = \frac{\mu_w}{\mu_b}\frac{(\rho_b - \rho_w)/\rho_w}{|dh/dx|} \tag{3}$$

Assuming the ratio of the viscosities is near unity and a maximum hydraulic gradient of 0.01, the ratio of vertical to horizontal velocity for the brines listed in Table 1 ranges from 5 for landfill leachate plumes to 33 for nuclear fuel reprocessing brines. This suggests that for concentrated waste brines and some remediation fluids, transport will be predominately vertical with limited horizontal migration in homogeneous materials. This effect is magnified as the hydraulic gradient decreases.

[11] Figure 1 represents a conceptual model for dense fluid transport in the saturated zone during and after a release. The aquifer is represented as locally homogeneous and isotropic but with a lens and an aquitard having lower permeability. During the release (Figure 1a) the brine falls almost vertically through the aquifer, mounds up on the lens, and cascades over the edges of the lens and continues to fall until pooling on the confining layer. Long-term release from a surface source exposes the lens and the confining layer to the concentrated brine, and, depending upon the permeability of the lens and aquitard, some fluid will physically sink and some of the fluid components will diffuse into these regions. Some time after the release has stopped, the condition within the aquifer is represented in Figure 1b where there now exists pools of dense fluid within the lens and in pockets within the confining layer. Contaminants dissolved within the dense fluid are released into the flowing groundwater by molecular diffusion through the stagnant water followed by advection and dispersion within the aquifer [*Flowers and Hunt*, 2000]. Similar transport and release scenarios are expected following the subsurface injection of water-miscible fluids for remediation purposes, and in some cases, their subsequent recovery.

3. Background

[12] The literature on brine transport in the subsurface is extensive and this section will only review aspects relevant to the vertical transport of brines and their subsequent recovery. In anticipation of the experimental program to follow, the density and viscosity of $CaCl_2$ and KCl brines are plotted in Figure 2. For both $CaCl_2$ and KCl, the densities increase nearly linearly up to the solubility limit for each salt. On the other hand, $CaCl_2$ viscosity increases nonlinearly from 1 to 9 cP (1 cP = 10^{-2} g cm^{-1} s^{-1} or 10^{-3} Pa s) while the KCl viscosity is nearly independent of salt concentration.

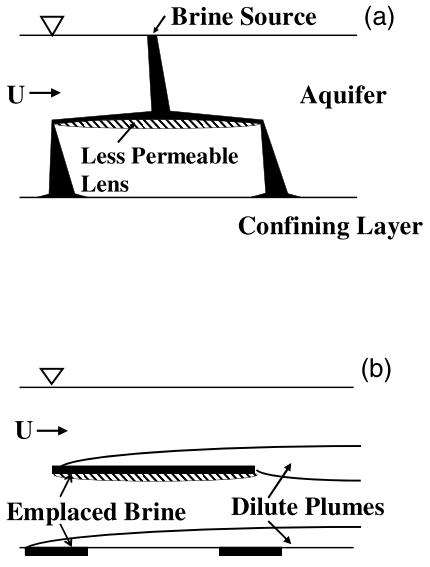

Figure 1. Brine transport in the subsurface (a) during a continuous release, the brine rapidly sinks through aquifer and (b) after release has ceased, brine is emplaced in less permeable regions and dilute groundwater plumes are formed.

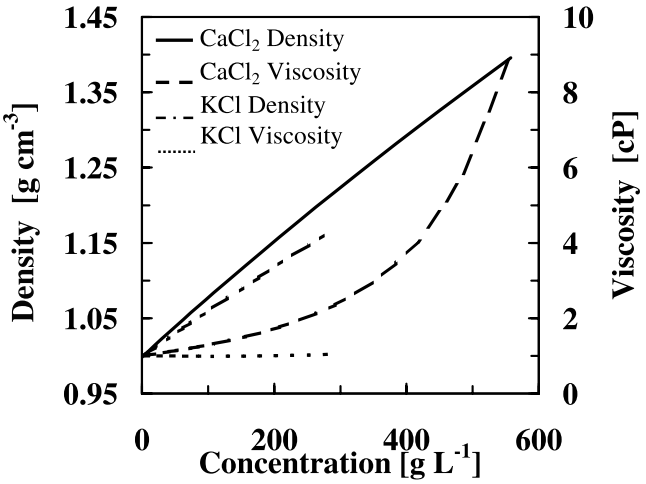

Figure 2. Density and viscosity of concentrated $CaCl_2$ and KCl solutions [*Lide*, 2000].

[13] Various observational and modeling studies have examined brine mixing with freshwater in porous media. Much of this effort has focused on a dense fluid introduced above a lighter fluid flowing horizontally where gravitational instabilities in the flow field generated descending bulbs or fingers of dense fluid. These gravitational instabilities were studied by *Lapwood* [1948] for a heated fluid at the base of the porous medium and then by *Wooding* [1959] for solute-induced density differences. This earlier work was followed by the theoretical and experimental contributions of *List* [1965] on density-induced instabilities and then the extensive work that followed by *Schincariol and Schwartz* [1990] and *Oostrom et al.* [1992]. These researchers selected experimental conditions where the brine-induced vertical velocity was generally much less than the horizontal velocity. Most of List's experiments were conducted with $U_b/U_x < 0.1$, *Schincariol and Schwartz* [1990] adopted experimental conditions where $U_b/U_x < 1.9$. *Oostrom et al.* [1992] experiments covered the range of 0.1 to 2.6 in U_b/U_x and they recognized the importance of this dimensionless velocity ratio. *Simmons et al.* [2002] provided visualizations of dense fluid migration as fingers when there was no horizontal flow in water-saturated porous media. When spatially heterogeneous porous media were examined, there was additional complexity in the observed flow field [*Schincariol and Schwartz*, 1990; *Swartz and Schwartz*, 1998; *Barth et al.*, 2001]. For dense fluids described in Tables 1 and 2 and the emplacement conditions depicted in Figure 1a, mixing during vertical transport will dominate over horizontal advection.

[14] There are four approaches considered below to modeling brine mixing with freshwater during vertical transport. First, mixing is modeled as a dispersion process between two fluids with a significant concentration difference and thus a density contrast. Second, mixing is represented as fingering phenomena between two fluids with a viscosity contrast. Third, a stability analysis is utilized that accounts for both the density and viscosity contrasts. Finally, there is numerical modeling that includes multiple processes and more complex geometry.

3.1. Dispersion

[15] The one-dimensional advection-diffusion equation for a dissolved, conservative compound is represented in porous media as

$$\frac{\partial C}{\partial t} = -U\frac{\partial C}{\partial z} + D_{pm}\frac{\partial^2 C}{\partial z^2} \tag{4}$$

where C is the mass concentration, U is the pore water velocity, and the dispersion coefficient, D_{pm}, is taken as a linear combination of molecular and hydrodynamic factors through

$$D_{pm} = \frac{D_{mol}}{\tau} + \alpha_L U \tag{5}$$

where D_{mol} is the molecular diffusivity, τ is the tortuosity correction factor that takes on values near 1.4 for granular porous media, and α_L is the longitudinal dispersivity. For laboratory experiments in homogeneous, isotropic porous media, *Perkins and Johnston* [1963] and *Fried and Combarnous* [1971] agreed that α_L is directly proportional to the medium grain size, d_g, giving

$$D_{pm} = \frac{D_{mol}}{\tau} + 1.75 d_g U \tag{6}$$

For 1 mm sand grains and a velocity of 1 m d^{-1}, the molecular diffusion contribution to overall dispersion is only one percent and can be neglected. Fick's law relates the dispersive flux to the concentration gradient. The experimental and theoretical contributions of *Hassanizadeh and Leijnse* [1988, 1995], *Schotting et al.* [1999], and *Watson et al.* [2002] question whether the dispersive flux is linearly dependent upon the concentration gradient. They formulate a nonlinear dispersive flux expression that reduces to Fick's law at low salt concentrations, but as *Schotting et al.* [1999] state, the formulation is not mechanistically linked to the physical processes causing dispersion.

[16] For a step function change in the influent concentration from C_i to C_o at $t = 0$, the concentration at downstream location x is [*Freeze and Cherry*, 1979]

$$\frac{C(x,t) - C_i}{C_o - C_i} = \frac{1}{2}\left[erfc\left(\frac{x - Ut}{2\sqrt{D_{pm}t}}\right) + \exp\left(\frac{Ux}{D_{pm}}\right) erfc\left(\frac{x + Ut}{2\sqrt{D_{pm}t}}\right)\right] \tag{7}$$

In most cases, the second term within the brackets provides a small contribution and is dropped.

[17] *Perkins and Johnston* [1963] and *Fried and Combarnous* [1971] both considered the influence of density and viscosity contrasts on dispersion. The porous media dispersion coefficient, D_{pm}, compared to the dispersion coefficient for a dilute tracer, D_T, is a bulk representation of the influence of the brine properties on mixing processes. *Wood et al.* [2004] argue against the application of advection-dispersion models for breakthrough curve analyses during unstable vertical displacements. *Menand and Woods* [2005] report a transition from dispersive transport enhanced over tracer dispersion at moderate gravitational instabilities to constant velocity fingers that could not

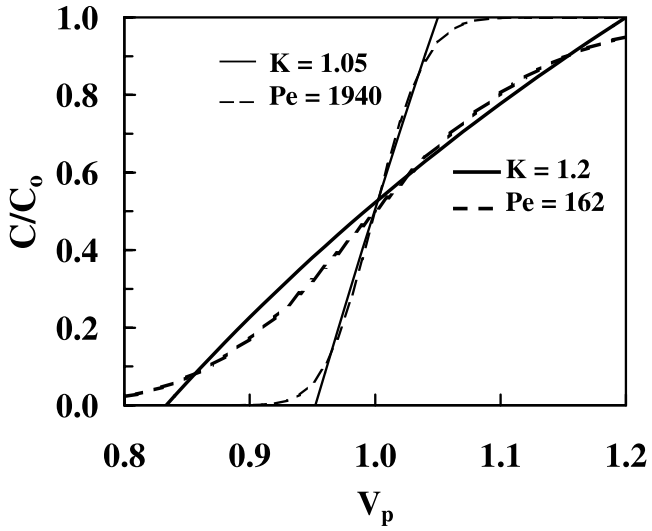

Figure 3. Comparison of breakthrough curves predicted by Koval's model and the corresponding best fit to the advection-diffusion equation for a step input.

be represented as dispersive. The experimental data collected by *Schotting et al.* [1999], *Watson et al.* [2002], and *Menand and Woods* [2005] are included in a later analysis of brine properties on dispersion.

3.2. Viscous Fingering

[18] An alternative approach to modeling miscible displacement as a dispersive process is to examine the viscosity contrast between the two fluids and model mixing as viscous fingering. This approach has considerable following in the petroleum reservoir engineering community where petroleum recovery is promoted by the injection of miscible and immiscible fluids of dramatically different viscosities. Comprehensive reviews of the importance of viscosity in miscible displacements are available [*Stalkup*, 1983; *Homsy*, 1987; *Lake*, 1989], and the key parameter is the mobility ratio, M, simplified here as the ratio of the resident fluid viscosity, μ_R, to the displacing fluid viscosity, μ_D,

$$M = \frac{\mu_R}{\mu_D} \tag{8}$$

When the resident fluid is less viscous than the displacing fluid, $M < 1$, stable displacements are observed since fingering is suppressed at the interface between these fluids. However, when the resident fluid is more viscous, $M > 1$, the displacing fluid can finger into the resident fluid and the displacement is unstable. The mobility ratio figures prominently in the numerous viscous fingering models that have been reviewed by *Sorbie et al.* [1995].

[19] For one-dimensional displacements in relatively homogeneous porous media, a model by *Koval* [1963] can accurately predict effluent concentration profiles. Koval's model adopted concepts from the *Buckley and Leverett* [1942] fractional flow formulation to arrive at the normalized effluent concentration in terms of a single parameter, $K > 1$:

$$\frac{C(V_p)}{C_o} = \frac{K - \sqrt{\frac{K}{V_p}}}{K - 1} \tag{9}$$

where $C(V_p)$ is the effluent concentration after V_p pore volumes of displacing fluid have been injected at a concentration of C_o, and K is given by

$$K = HE \tag{10}$$

where H is an empirical parameter representing column heterogeneity determined from a tracer test, and E is an effective mobility ratio. The effective mobility ratio utilized the quarter power mixing rule for determining the viscosity of miscible fluids. Koval determined that a reasonable composition of the fluid in the mixing zone was 78% resident fluid and 22% displacing fluid. Under these conditions, Koval's effective mobility ratio becomes

$$E = \left(0.78 + 0.22M^{1/4}\right)^4 \tag{11}$$

There is a similarity between Koval's model of breakthrough and that predicted by the solution to the advection-dispersion model. Koval's solution predicts zero effluent concentration until $V_p = 1/K$ and 100% breakthrough when $V_p = K$. Simplifying equation (7) to include only the first term on the right hand side, setting $x = L$, as the column length, letting $C_i = 0$, and expressing the result in terms of pore volumes, $V_p = Ut/L$, the advection-dispersion solution becomes

$$\frac{C(V_p)}{C_o} = \frac{1}{2} erfc\left(\frac{1 - V_p}{2\sqrt{V_p/Pe}}\right) \tag{12}$$

where Pe is a column Peclet Number given by UL/D_{pm}. As indicated in Figure 3 for two different conditions, the Koval solution for fingering is similar to the error function solution representing dispersion at least over the range $0.1 < C/C_o < 0.9$. In many cases dispersion coefficients are determined from times when 5% and 95% of the influent concentrations are reached rather than fitting a complete breakthrough curve. Koval coefficients are similarly determined from extrapolated "breakthrough efficiencies" when the displacing fluid first appears ($V_p = 1/K$) and "recovery efficiencies" when the 100% of the effluent first becomes the displacing fluid ($V_p = K$). Thus breakthrough curves can be modeled as diffusive or fingering with a single parameter, D_{pm} or K. From assumed values of the Koval parameter, fitted values of the Peclet number were determined that most closely aligned with the point $C/C_o = 0.90$. By repeating the process represented in Figure 3 for $1.01 < K < 2.0$, there is a 1 to 1 correspondence between these two parameters for mixing, and the resulting empirical relationship between these parameters is

$$\frac{1}{Pe} = \frac{D_{pm}}{UL} = 0.11(K - 1)^{1.79} \tag{13}$$

List [1965] introduced the concept of interface stability when perturbed with different wavelengths. *Schincariol et al.* [1994] demonstrated through simulations that for a given density difference, larger disturbing wavelengths are unstable and generate fingers while smaller wavelengths were stable. As the density difference increased, the

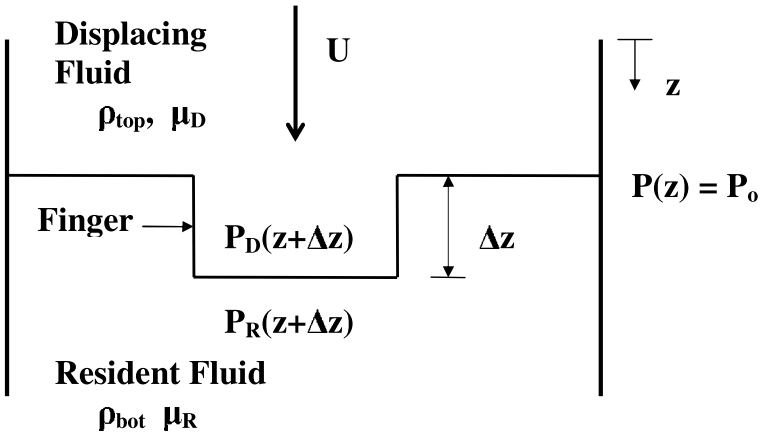

Figure 4. Hill's stability analysis for miscible displacement assuming flow is downward and a finger of the displacing fluid has propagated a distance Δz into the resident fluid.

unstable region moved to smaller wavelengths. *Menand and Woods* [2005] experimentally determined that the transitional wavelengths separating stable from unstable become smaller as the density difference increases. These numerical and experimental results suggest that column diameter can experimentally determine the transition to finger instabilities since only disturbance wavelengths less than the order of the column diameter are feasible.

3.3. Gravitational and Viscous Stability Analysis

[20] As suggested by the properties of the $CaCl_2$ brine at high concentrations, both density and viscosity contrasts will likely determine the mixing behavior as the brine sinks through an aquifer. *Hill* [1952] provided a stability analysis for such a system where the original application was the adsorption of colored compounds onto activated carbon from concentrated sugar solutions. Column mixing was of concern when freshwater was displaced by sugar solutions and when sugar solutions were displaced by a freshwater solution to recharge the activated carbon adsorption sites. Given the different notation used by Hill and the importance of this result to the analysis that follows, the stability analysis is repeated here. *Saffman and Taylor* [1958] also asserted the stability criterion, and it has been used in various forms by many investigators.

[21] Figure 4 represents downward flow at a pore water velocity U of a displacing fluid having a viscosity of μ_D with the resident fluid at viscosity μ_R. In anticipating a generalization of the result to follow, the fluid density on the top is denoted as ρ_{top} and the density of the fluid on the bottom is ρ_{bot}. The interface between these two fluids is initially sharp but is then perturbed downward a distance Δz in a small section. The condition for stability is that the resident fluid within the disturbance has a higher, restoring pressure

$$P_R(z+\Delta z) \quad > \quad P_D(z+\Delta z) \tag{14}$$

Darcy's law is then applied to the vertical flow in both fluids using

$$U = -\frac{k}{n\mu}\left[\frac{\Delta P}{\Delta z} - \rho g\right] \tag{15}$$

and this provides estimates for the fluid pressures on both sides of the disturbed interface at location $z + \Delta z$:

$$P_o + \left(-\frac{n\mu_R}{k}U + \rho_{bot}g\right)\Delta z \quad > \quad P_o + \left(-\frac{n\mu_D}{k}U + \rho_{top}g\right)\Delta z \tag{16}$$

Simplifying and taking U as positive for downward flow, this stability criterion becomes

$$\frac{kg\left(\rho_{bot} - \rho_{top}\right)}{n\mu_D U} > \frac{\mu_R - \mu_D}{\mu_D} \tag{17}$$

The derivation can be repeated for a coordinate system with z and U both positive upward, and the same result is obtained. The stability criterion is represented in a more compact notation by noting that the left hand side of equation (17) is the ratio of the buoyancy-induced pore water velocity to the magnitude of the imposed pore water velocity, and this ratio is defined as the gravity number, N_G:

$$N_G \equiv \frac{kg\left(\rho_{bot} - \rho_{top}\right)}{n\mu_D|U|} \tag{18}$$

The absolute value of the velocity indicates the velocity is always positive and the sign of the gravity number is determined by the difference in bottom and top fluid densities. In this way, positive gravity numbers have a gravitationally stable interface since $\rho_{bot} > \rho_{top}$.

[22] Hill's criterion for stable miscible displacement in equation (17) in terms of the gravity number and the mobility ratio becomes

$$N_G > M - 1 \tag{19}$$

This criterion is a compact method to identify regions of stability and instability in four regions of N_G and M space as illustrated in Figure 5 where the dashed line represents the critical gravity number, $N_{G,c} = M - 1$. Region I ($N_G > 0$, $M > 1$) is conditionally stable since displacements are stabilized by gravitational forces, but are destabilized by the viscosity contrast. Region II ($N_G > 0$, $M < 1$) is

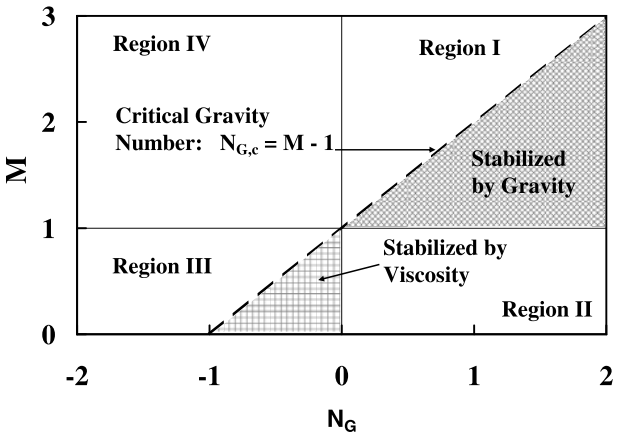

Figure 5. Miscible displacement regions including Hill's criterion for stability.

inherently stable, with displacements stabilized by both gravity and viscosity. Region III ($N_G < 0$, $M < 1$) is conditionally stable, but now displacements are destabilized by gravitational forces and stabilized by the viscosity contrast. Region IV ($N_G < 0$, $M > 1$) is inherently unstable since displacements are destabilized by both gravity and viscosity. For brine/freshwater systems where the viscosity and density both usually increase with salt concentration, upward flows are either stable in region II or unstable in region IV, while downward flows are conditionally stable in regions I and III. This representation is an alternative to formulas for the critical velocity for stable displacements presented by *Saffman and Taylor* [1958], *Fried and Combarnous* [1971], *Welty and Gelhar* [1991], and others where there are somewhat awkward sign conventions or restrictions on flow directions.

3.4. Numerical Approaches

[23] Given the importance of density-driven flow within two- and three-dimensional porous media systems and the need to represent heterogeneities, numerical modeling efforts have been extensive. *Frind* [1982] provides an early summary of numerical efforts and describes some of the challenges in implementing transient solution procedures. The model formulation assumed salt dispersion could be described by fixed values of the longitudinal and transverse dispersivities and a constant fluid viscosity. The steady state Henry problem for seawater intrusion was recognized as being useful for model comparisons, but it was unrealistic in its assumption of a constant dispersion coefficient. The concern about nuclear waste storage within salt domes lead to an extensive modeling effort referred to as the HYDROCOIN project that undertook model comparisons for groundwater flow over an exposed salt dome. *Herbert et al.* [1988] describes one such numerical model that incorporated fluid density dependence on salt concentration, a constant viscosity, and either constant dispersion coefficients or constant dispersivities for the medium. In contrast, *Welty and Gelhar* [1991, 1992] recognize that fluid density and viscosity are variables that determine the macroscopic dispersion in their simulation of a heterogeneous porous medium and this is expanded upon by *Barth et al.* [2001]. *Kolditz et al.* [1998] provides an updated summary of the numerous numerical models available for simulating variable density groundwater flows.

[24] There is recognition that the modeling results depend on the numerical solution procedures and the model representation of the subsurface. Numerical solution methods generate perturbations that result in instabilities in the simulated flow field [*Schincariol et al.*, 1994]. Predicted flow fields also depend on random perturbations imposed on the boundaries [*Simmons et al.*, 1999], on small perturbations in the porous media properties [*Schincariol*, 1998], and on truncation and round-off errors [*Liu and Dane*, 1997; *Mazzia et al.*, 2001]. *Simmons et al.* [2001] in their review and look forward emphasize the challenges in representing realistic heterogeneities in numerical models. *Diersch and Kolitz* [2002] and *Oswald and Kinzelbach* [2004] provide comprehensive reviews of transport models for variable density flows and comment on the need for benchmark experiments to permit the comparison of model results with experimental observations rather than comparison only among simulation results.

[25] The petroleum engineering community has engaged in extensive modeling of miscible displacement where viscous and gravitational forces must both be included. *Manickam and Homsy* [1995] simulate fingering instabilities and in particular note that initially diffuse interfaces between miscible fluids can alter interfacial stability compared to predictions based on initially sharp interfaces. Multidimensional finger propagation is the norm in petroleum engineering reservoir applications, and *Riaz and Meiburg* [2003] explore the stability of interfaces in the typical "five-spot" pattern. The modeling of geothermal resources explores many of these same questions, but there is the added complexity associated with temperature gradients. *Oldenburg and Pruess* [1998] present a model formulation for thermohaline convection as encountered in hypersaline geothermal systems having brine concentrations of 25 weight percent and temperatures up to 300°C. This modeling effort required accounting for the dependency of fluid density and viscosity on both brine concentration and temperature.

[26] *Roeder and Falta* [2001] investigate the challenges in modeling the one-dimensional injection of water-miscible alcohol solutions for NAPL dissolution and the subsequent displacement of the alcohol fluids. Through adjustment of the upward flow velocities, the displacements could be made stable as well as unstable using a stability analysis similar to that of Hill. One-dimensional advection-dispersion models had fitted dispersion coefficients that were dependent upon the stability of the displacement and they demonstrate the capability of the University of Texas Chemical Flooding simulator (UTCHEM) to adequately predict mixing processes due to density and viscosity contrasts.

4. Literature Data

[27] Given the importance of density-driven flow in porous media, there have been many experimental studies that quantify dispersion at miscible displacement fronts when there are density and/or viscosity contrasts in the two fluids. A search through the literature identified a number of these studies were it was possible to determine or estimate the experimental parameters, N_G and M and normalized dispersion D_{pm}/D_T. The experimental conditions and necessary assumptions needed to arrive at parameters are described in Appendix A, and the numerical values for

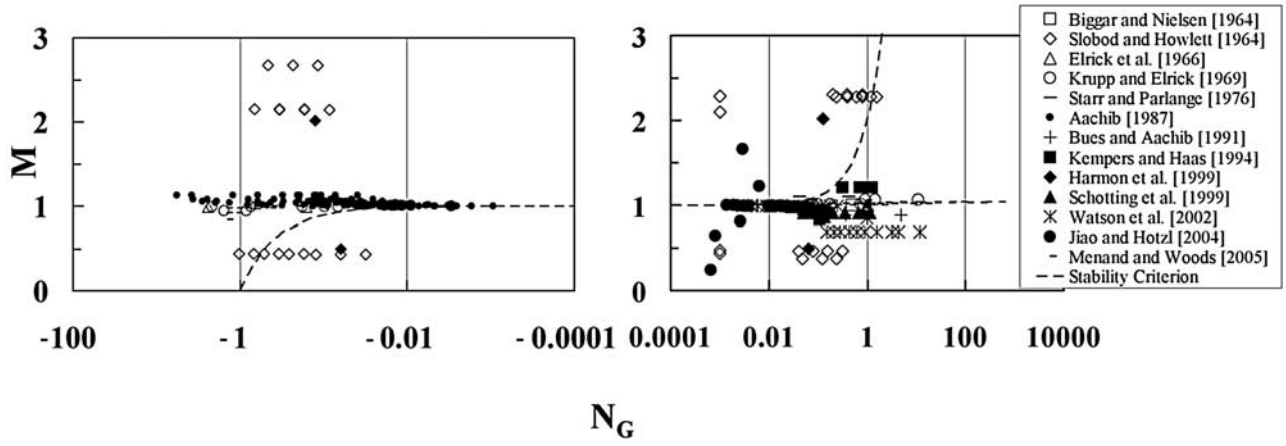

Figure 6. Hill's stability criterion compared with the mobility ratios, M, and the gravity numbers, N_G, for experimental results reported in the literature for vertical miscible displacements.

each of the 379 experimental results are available in the auxiliary material[1]. The experimental conditions for these empirical studies are classified on the Hill criterion stability diagram in Figure 6. In order to visually represent the experimental conditions, a linear scale for mobility ratio is plotted against the log of the gravity number, unlike the linear scaling in Figure 5, so that the critical gravity number, $N_{G,c}$, separating stable from unstable conditions as predicted by Hill is now represented by a dashed curve. Experimental interest in brines has largely focused on upward flow which restricted the investigations to region II ($N_G > 0$, $M < 1$; always stable) and region IV ($N_G < 0$, $M > 1$; always unstable). Within regions I and III, fewer data sets are available and only *Slobod and Howlett*'s [1964] data span across the stability criterion.

[28] Literature data on dispersion coefficients normalized by tracer dispersion coefficients, D_{pm}/D_T, are plotted in Figure 7 as a function of the gravity number. Figures 7a and 7b compile the available data for negative and positive gravity numbers, respectively. For N_G less negative than about -0.05, dispersion is similar to tracer dispersion. At more negative values of N_G, normalized dispersion dramatically increases. Even though *Wood et al.* [2004] and *Menand and Woods* [2005] question the use of dispersion models at gravity numbers more negative than approximately -1, these results are included for completeness. As summarized earlier, small column diameters are expected to suppress larger disturbances, but there is no evident effect of column diameter in Figure 7a where column diameters ranged from 2.1 cm to 20.6 cm. The experimental results that show the greatest dispersion were obtained by *Starr and Parlange* [1976] and *Aachib* [1987] with column diameters of 6.0 and 5.0 cm, respectively. In contrast the smallest normalized dispersion was obtained by *Elrick et al.* [1966] and *Krupp and Elrick* [1969] where the column diameters were 9.5 cm. *Menand and Woods* [2005] utilized a rectangular cross section that was 1.0 cm by 15.0 cm where the narrow dimension could have suppressed instabilities.

[29] Only the *Slobod and Howlett* [1964] data suggest the importance of the mobility ratio where data for $M \approx 2$ have $D_{pm}/D_T > 100$ while for $M \approx 0.5$ the trend is an increase in dispersion over the range $-1 < N_G < -0.1$. For positive gravity numbers there is a general trend in Figure 7b for $D_{pm}/D_T \approx 1$ when $N_G < 0.1$, and decreasing D_{pm}/D_T for $N_G > 0.1$. The exceptions to this trend in Figure 6 (right) are data from *Slobod and Howlett* [1964] that indicate viscous-induced instabilities for $N_G < 1$ where D_{pm}/D_T approaches 100. For their M $\approx$ 0.5 data, normalized dispersion coefficients are similar to those reported by others. The reason for the dramatically different results of the *Slobod and Howlett* [1964] data is not certain, although this is one of the few data sets that utilized organic solvents to manipulate density and viscosity rather than using aqueous brines. *Grubb and Sitar* [1999] identify the importance of the nonmonotonic behavior of viscosity with alcohol concentration during cosolvent flooding for NAPL removal. For equal volume mixtures of some alcohols with water, the liquid viscosity can be 3 to 4 times that of the end-member viscosities, completely unlike the behavior of brines illustrated in Figure 2. If this nonmonotonic viscosity occurs under Slobod and Howlett's experimental conditions, then characterization of the displacement by the end-member mobility ratios is misleading.

[30] The earlier researchers did not select these experimental conditions for testing Hill's stability criterion in regions I and III where viscous and gravitational forces are in opposition. In addition, there is considerable variability among reported experimental results and this suggests the need for additional experimental data.

5. Experimental Program

[31] A one-dimensional laboratory-scale experimental program was designed to investigate if Hill's stability criterion characterizes column dispersion and to quantify the effect of mobility ratio and gravity number on dispersion. This section summarizes the procedures and apparatus with greater detail provided by *Flowers* [2003]. The experiments examined the downward displacement of water by brine and brine displacement by water to specifically determine mixing processes in conditionally stable regions I and III noted in Figure 5 where gravitational and viscous forces are in opposition.

[1]Auxiliary materials are available at ftp://ftp.agu.org/apend/wr/2005wr004773.

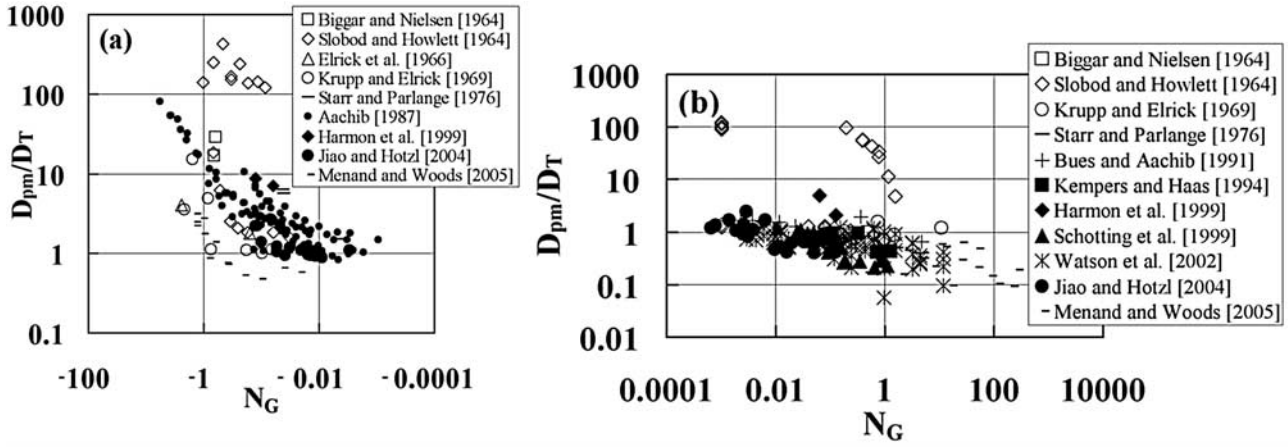

Figure 7. Normalized dispersion coefficients obtained from the literature: (a) negative gravity numbers and (b) positive gravity numbers.

[32] Figure 8 is a schematic of the experimental apparatus employed in this investigation. The brine and freshwater were held in constant head 50-L Mariotte bottles and the fluid flow rate was maintained by a pulseless flow pump with the flow rate determined manually. Three different porous medium columns were utilized to achieve a range in gravity numbers. The columns were wet packed in 1 cm lifts by sprinkling sand through water, vibrating the whole system, and compacting with a steel rod [*Oliviera et al.*, 1996]. Stainless steel disks were placed at the inlet and outlet of the columns to achieve plug flow entrance and exit conditions, and tracer tests with the disks flush against each other gave dispersion coefficients much less than column dispersion coefficients. Column characteristics are given in Table 3. The column effluent was passed through a small volume where conductivity was measured using a Jenway model 1440 meter with a conductivity sensor having a cell constant of approximately 10 cm^{-1}. Conductivity was recorded every 5 s and salt concentration was determined through a calibration process that recognized the nonlinear relationship between conductivity and the salt concentrations used in these experiments.

[33] A typical experiment involved three displacement cycles, where a displacement cycle consisted of approximately three pore volumes of brine displacing the resident freshwater, followed by three pore volumes of freshwater displacing the resident brine. For each flow rate, or after three displacement cycles, the porous media column was degassed by back flushing with carbon dioxide followed by deionized water. The carbon dioxide was at a pressure of approximately 70 kPa and was followed by approximately 10 pore volumes of deionized water to dissolve any residual CO_2 gas.

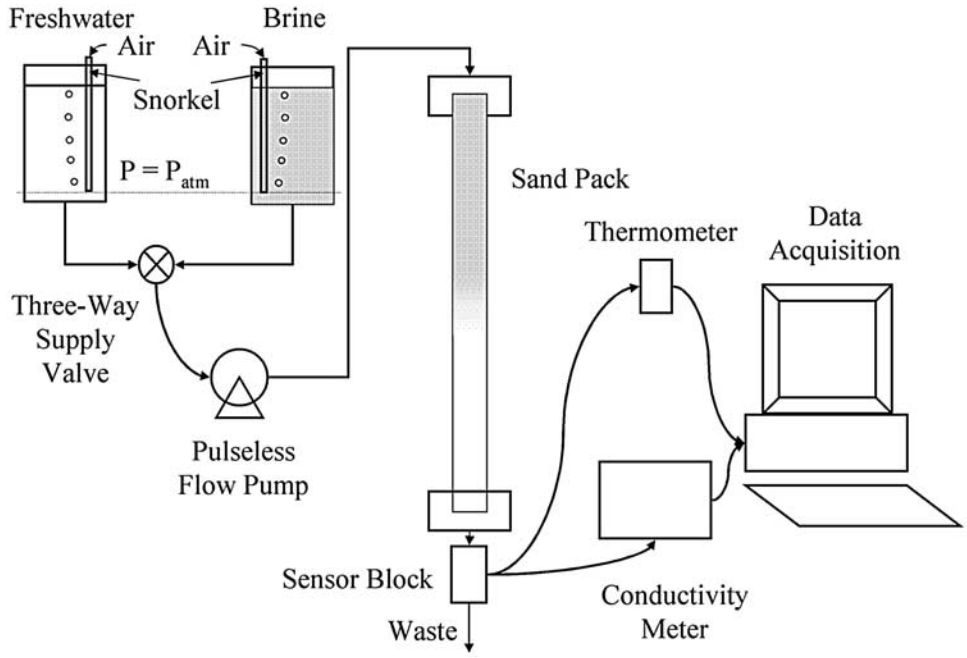

Figure 8. Apparatus for downward flow tracer and miscible displacement experiments.

Table 3. Column Properties

Column Description	Inside Diameter, cm	Length of Sand Pack, cm	Grain Diameter, mm	Permeability, 10^{-8} cm^2	Porosity
Small	3.19	97.1	0.5	92.5 ± 0.7	0.382
Lower k large diameter	5.78	98.2	0.5	91.9 ± 0.2	0.366
Higher k large diameter	5.78	96.3	1.0	353 ± 2	0.342

[34] The data were used to develop an unbiased estimate of U and D_{pm} by fitting the measured raw data to the one-dimensional advection-diffusion solution appearing in equation (12). The parameters U and D_{pm} were determined by an iterative technique that produced a minimum of the sum of the squared differences between measured data and model predictions [*Toride et al.*, 1999]. Several artificial concentration data sets were generated using various specified values of U and D_{pm} and the iterative technique arrived at the actual values with an error less than 0.01%. Model estimated pore water velocity was usually within 2% of the measured velocity.

[35] The mixing behavior in the three columns without density and viscosity contrasts was determined using a series of tracer displacement experiments with calcium chloride solutions of 0.1 and 0.2 g L^{-1}. For each column, three experimental cycles were completed at various flow rates that covered the entire range of the pump. Tracer dispersion for all three columns is presented in Figure 9 and the dispersion coefficients were fitted to a power function of the velocity. The dispersion coefficients had a velocity dependence to a power slightly greater than 1 rather than the anticipated linear dependence given in equation (6).

[36] Calcium chloride and potassium chloride were chosen as experimental brines because of their high solubility and different dependence of viscosity on salt concentration as indicated in Figure 2. Because of limitations of the conductivity meter, 263 g L^{-1} was the maximum calcium chloride concentration utilized. Table 4 summarizes the specific experimental conditions and the properties of the brines along with the mobility ratios and critical gravity numbers, $N_{G,c} = M - 1$ for the experiments. The gravity numbers and mobility ratios are plotted in Figure 10, indicating the selection of experimental conditions that span the stability criterion in both regions I and III.

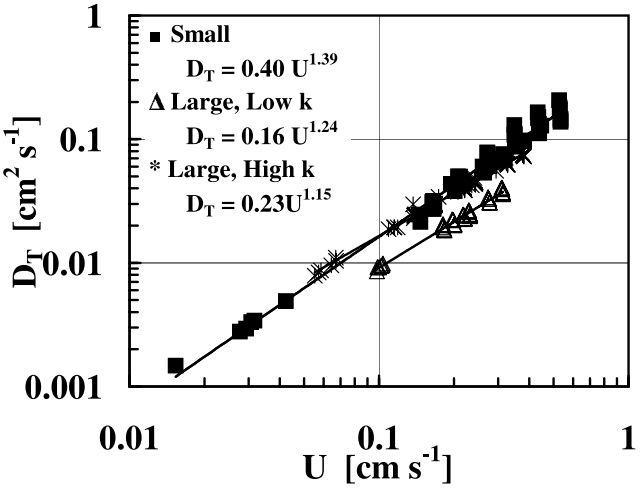

Figure 9. Dispersion coefficients obtained for dilute tracer tests in the three experimental columns.

6. Results and Discussion

[37] Results are reported for 382 experiments that quantified column dispersion where gravitational and viscous forces were at opposition. The experimental results are given first for region III under viscously stable ($M < 1$) but gravitationally unstable ($N_G < 0$) conditions, and then for region I with viscously unstable and gravitationally stable flows ($M > 1$; $N_G > 0$). All breakthrough curves are available from *Flowers* [2003], and the experimental data are available in the auxiliary material.

6.1. $N_G < 0$ Results

[38] Three breakthrough curves for negative gravity number experiments in Figure 11 illustrate the dependence of mixing processes on the mobility ratio and the gravity number. When the $CaCl_2$ concentration is fixed at 263 g L^{-1}, the mobility ratio is 0.47, and decreasing the flow velocity increases the gravity number from $N_G = -0.11$ to $N_G = -0.94$ with a corresponding increase in mixing compared to a dilute tracer. In contrast, for a gravity number of -0.11, there is little difference in the breakthrough curves for $CaCl_2$ with $M = 0.47$ and KCl with $M = 1.0$ even though the KCl displacement is expected to be unstable ($N_{G,c} = 0$) according to equation (19).

[39] Normalized dispersion coefficients for all gravitationally unstable conditions are plotted in Figure 12a. For gravity numbers less negative than -0.3, the dispersion coefficients are within a factor of three of the dispersion expected for dilute tracers. For gravity numbers more negative than -0.3 there is a consistent increase in dispersion with more negative gravity number. The results for gravity numbers from -2 to -1 are only approximated by one-dimensional dispersion coefficients since there are obvious instabilities arising from selective pockets of brine reaching the column exit. This observation is in agreement with *Menand and Woods* [2005], who report dispersion coefficients for gravity numbers only as negative as -1.4 (our definition) in what they refer to as a transition between dispersive and advective instabilities. The scatter in the normalized dispersion data in Figure 12a arises from greater normalized dispersions with the smaller experimental column diameter. This is opposite to the effect suggested by *Schincariol et al.* [1994] and *Menand and Woods* [2005] where instability suppression is expected in the smaller diameter column since only shorter disturbance wavelengths are possible.

[40] The mobility ratio contributes little to stabilizing displacements and this is illustrated in Figure 12b which includes only the large diameter, higher permeability column data. The 52.1 g L^{-1} $CaCl_2$ dispersion coefficients are in agreement with the values determined for KCl. When

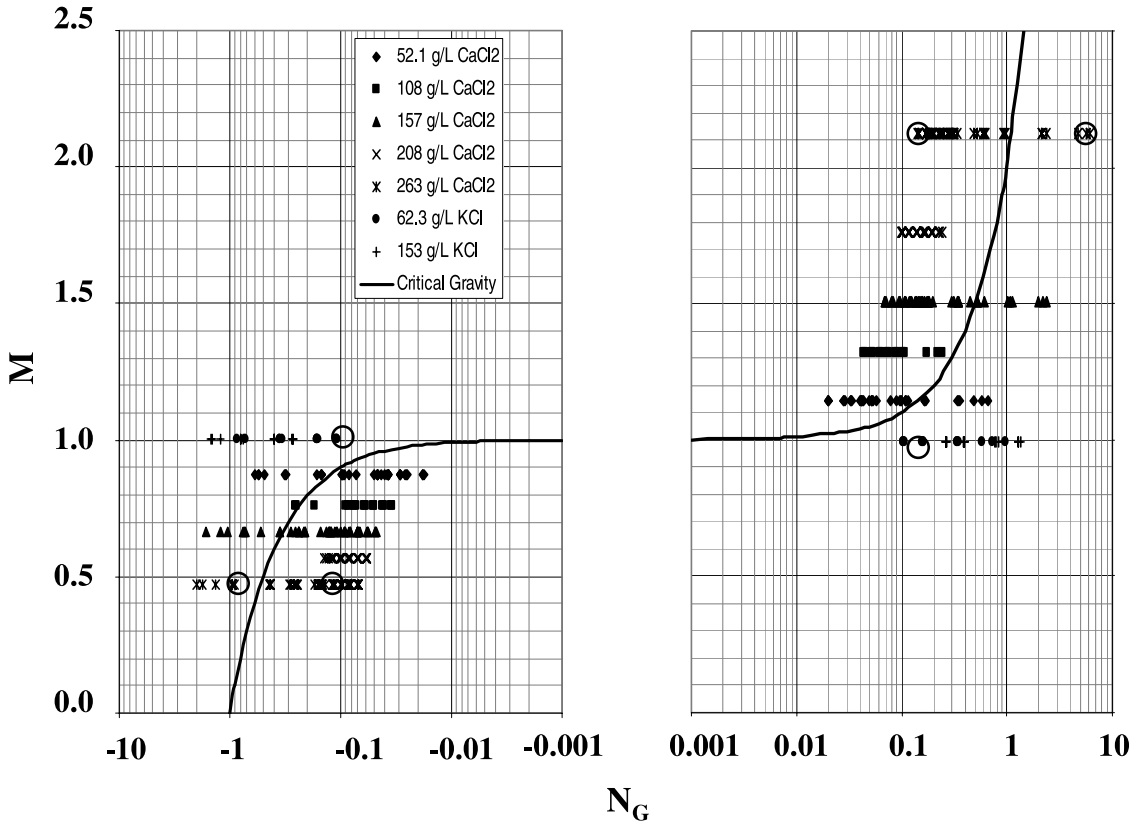

Figure 10. Hill's stability criterion compared with the mobility ratio, M, and the gravity number, N_G, for new downward flow experiments where negative gravity numbers correspond to brine displacement of water and positive gravity numbers are for water displacement of brines. Breakthrough curves are plotted for the circled points in Figure 11 for negative gravity numbers and in Figure 13 for positive gravity numbers.

$N_G > -0.3$ dispersion coefficients are close to those determined for dilute tracers, and the KCl and dilute $CaCl_2$ brines have increased dispersion for $N_G < -0.3$. Hill's predicted critical gravity number for 52.1 g L^{-1} $CaCl_2$ is -0.125 as indicated in Figure 12b, but the dispersion coefficients are still the same as those determined for KCl and dilute tracers over the range $-0.3 < N_G < -0.125$ suggesting that while instabilities are expected for $CaCl_2$, they are not detectable. In contrast, dispersion data for $CaCl_2$ brines at 157 and 263 g L^{-1} have a slightly larger interval of stable dispersion out to the predicted critical gravity numbers. Brine dispersion for the most negative gravity numbers ($N_G < -1.0$) are similar to that observed for the KCl brines. In comparing the literature data in Figure 7a with this new experimental data, there is general agreement that the transition to enhanced dispersion happens for $N_G \approx -0.3$, and these new data are

Table 4. Physical Properties of the Experimental Brines at 20°C From *Lide* [2000] and Experimental Conditions

Concentration, g L^{-1}	Density, g cm^{-3}	Dynamic Viscosity, cP	Brine Displacing Water		Water Displacing Brine	
			M	$N_{G,c}$	M	$N_{G,c}$
		$CaCl_2$ Brine				
52.1	1.040	1.14	0.875	−0.125	1.14	0.14
108	1.084	1.32	0.758	−0.242	1.31	0.31
157	1.120	1.51	0.663	−0.337	1.51	0.51
208	1.158	1.76	0.567	−0.433	1.76	0.76
263	1.198	2.13	0.470	−0.530	2.13	1.13
		KCl Brine				
62.3	1.037	0.99	1.0	0	1.0	0
153	1.091	0.99	1.0	0	1.0	0

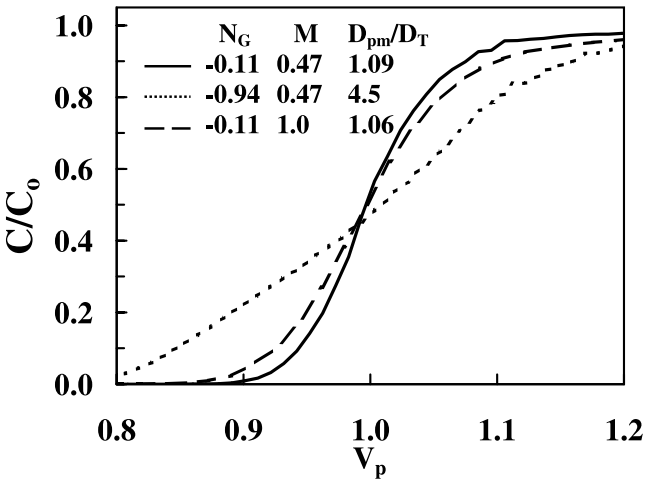

Figure 11. Breakthrough curves for the negative gravity number experimental conditions circled in Figure 10.

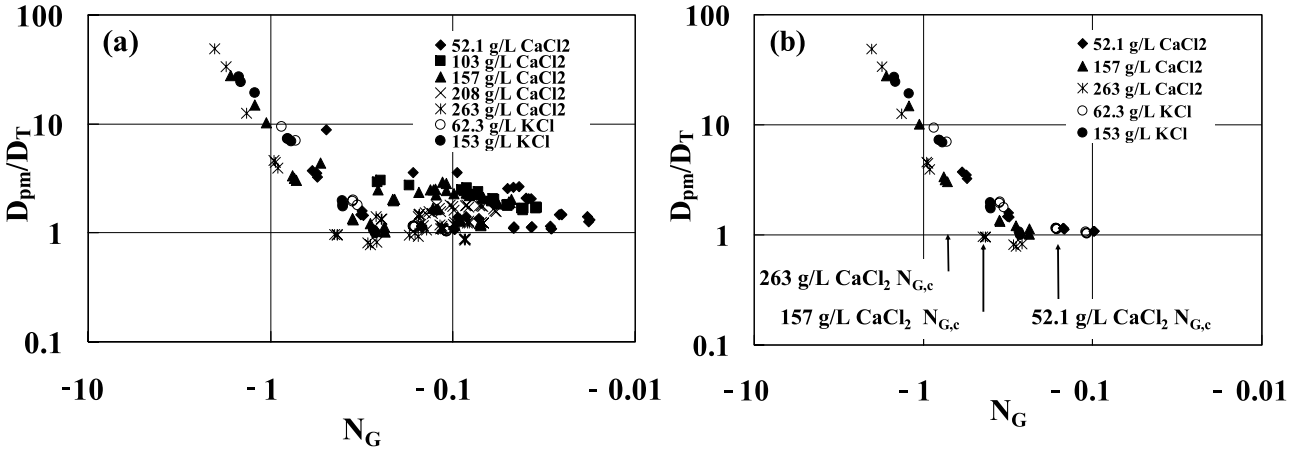

Figure 12. Normalized dispersion coefficients for negative gravity number results: (a) the complete data set and (b) only those data collected in the large diameter, higher-permeability column.

in agreement with the prior data with one exception. The *Slobod and Howlett* [1964] data for $N_G < 0$ and $M > 1$ represents conditions encountered in region IV where both gravity and viscosity are destabilizing and it is expected that normalized dispersion should be large.

6.2. $N_G > 0$ Results

[41] In region I ($N_G > 0$, $M > 1$), there is the trade-off between gravitational stabilization and viscous instability as illustrated by three breakthrough curves in Figure 13. For the KCl brine with $N_G = 0.16$ and $M = 1$, column dispersion is 73% of tracer dispersion as expected since $N_G > N_{G,c} = 0$. The displacement of the $CaCl_2$ brine at a similar gravity number of 0.14 has a fitted dispersion coefficient 2.6 times that of the dilute tracer since $N_G < N_{G,c} = 1.13$ or gravitational stabilization does not overcome viscous instability. When the gravity number for the concentrated $CaCl_2$ brine is increased to 6.2 ($N_G > N_{G,c} = 1.13$), dispersion is suppressed to a level that is only 38% of the value for a dilute tracer. These examples illustrate that Hill's stability criterion qualitatively describes the transition under positive gravity number conditions. The dashed breakthrough curve in Figure 13 for $N_G = 0.14$ suggests that advective instabilities are likely dominant and a dispersive model is only approximate.

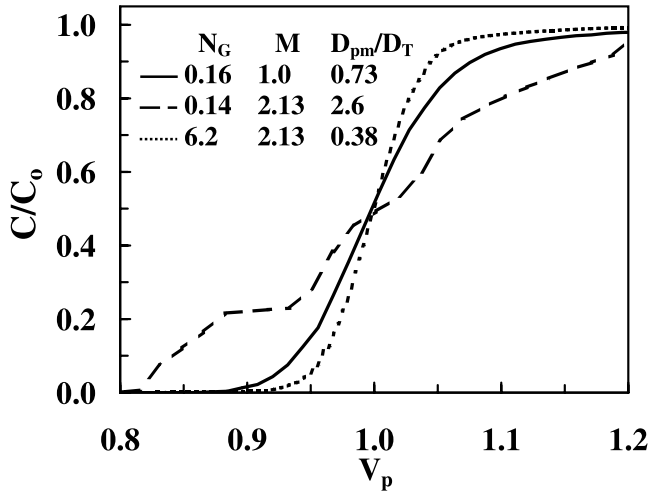

Figure 13. Breakthrough curves for positive gravity number experimental conditions circled in Figure 10.

[42] All normalized dispersion coefficients are plotted against gravity number in Figure 14a. For gravity numbers greater than about 1, the dispersion coefficients are approximately half that of dilute tracers as observed in the literature data (Figure 7b). For the KCl brines the normalized dispersion coefficient remains at about 75% the dilute tracer dispersion coefficient even as the gravity number approaches zero. Increased dispersion is seen for the $CaCl_2$ brines as the gravity number decreases with the increase attributed to viscous instabilities at the higher brine concentrations. A subset of $N_G > 0$ data is included in Figure 14b that covers the full range in $CaCl_2$ concentrations but does not include two of the intermediate concentrations. The dispersion data for 52 g L^{-1} $CaCl_2$ is relatively independent of gravity number and is similar to the KCl brine results since both have mobility ratios near 1. For the 157 g L^{-1} $CaCl_2$ brine having a mobility ratio of 1.51 and a critical gravity number of 0.51, normalized dispersion coefficients for $N_G < N_{G,c}$ increase above the values observed for KCl as expected from Hill's stability criterion. Finally, for the 263 g L^{-1} $CaCl_2$ brine with a mobility ratio of 2.13, the critical gravity number, $N_{G,c} = 1.13$ marks the transition from density stabilized flow observed for the KCl brines and increased normalized dispersion when viscous instabilities dominate.

[43] In the limit of zero gravity number, Koval's model provides an estimate of the asymptotic normalized dispersion coefficient. The heterogeneity parameter, H, is determined from tracer tests where the corresponding Koval parameter is $K_T = H$ from equation (10) with the value of K_T is obtained from equation (13) using D_T at the highest flow velocity instead of D_{pm}. The overall Koval parameter, K, is estimated from equation (10) using the effective mobility ratio in equation (11). This value of K when substituted into equation (13) provides an estimate of D_{pm} ($N_G = 0$). The asymptotic values of the normalized dispersion coefficients are drawn as dashed lines in Figure 14b, but are only estimates with a factor of uncertainty of about 50% due to variations in tracer dispersion in the three different columns. Even with these uncertainties, the exper-

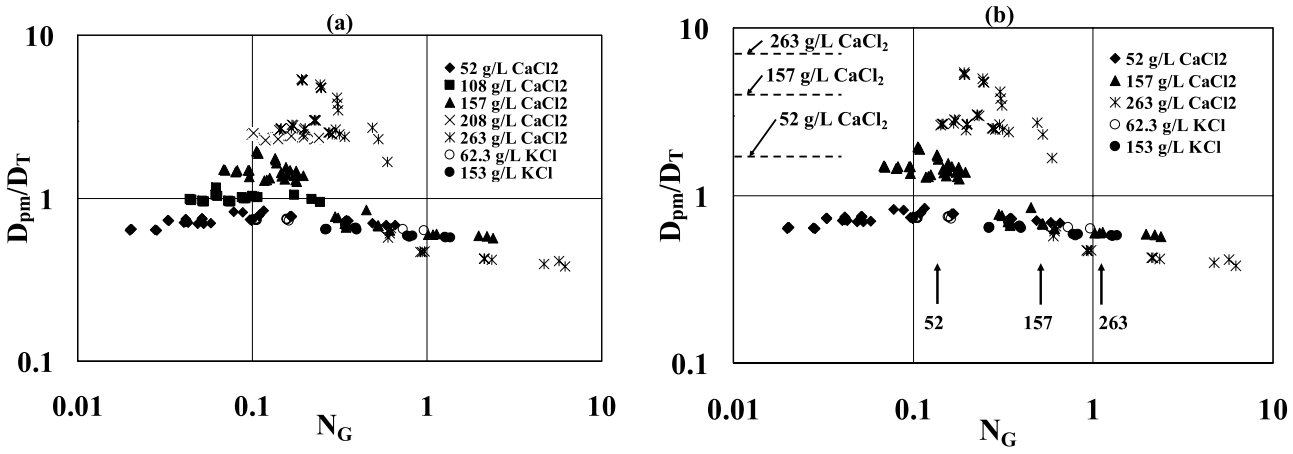

Figure 14. Normalized dispersion coefficients for positive gravity number results: (a) the complete data set and (b) selected $CaCl_2$ results noting the critical gravity number and the predicted asymptotic normalized dispersion from Koval's model with KCl results included for comparison. The vertical arrows labeled 52, 157, and 263 mark the critical gravity numbers for the corresponding $CaCl_2$ concentrations.

imental results suggest viscous instabilities develop near the critical gravity number predicted by Hill, and for gravity numbers an order of magnitude less than $N_{G,c}$, one-dimensional dispersion is approximated by Koval's model. The contribution of viscous fingering is not large and only increases dispersion coefficients at most by a factor of about 7 for the densest, most viscous brine at the highest flow velocities.

[44] Comparing Figure 14a with the literature data plotted in Figure 7b reveals general agreement that for $N_G > 1$, brine dispersion is reduced to about 50% of the value determined for tracers. However, the current experimental program has a wider range in mobility ratio to test Hill's stability criterion, and enhanced dispersion is observed for smaller values of the gravity number for the most concentrated brines. There is some evidence of this effect in one data point reported by *Harmon et al.* [1999] and perhaps a few measurements from *Jiao and Hötzl* [2004]. The experimental results of *Slobod and Howlett* [1964] remain an anomaly since when the mobility ratio is about 2, the dispersion coefficients increase to values 100 times that of a tracer as the gravity number falls below 1. As discussed above, one explanation for the *Slobod and Howlett* [1964] results is a possible nonmonotonic dependence of viscosity on solvent composition.

7. Application

[45] The synthesis of experimental data using stability analysis and correlations to the gravity number and mobility ratio permits the application of these results to other conditions. Experimental results on alcohol flooding for nonaqueous phase liquid (NAPL) displacement and subsequent alcohol recovery modeled by *Roeder and Falta* [2001] were not included within the current data compilation due to the complexity of multiple miscible fronts of water, alcohol, and NAPL. However, it is possible to estimate the dispersion when the alcohol emplacement front displaces water and the dispersion during the recovery of the alcohol when water displaces the alcohol. Table 5 summarizes the relevant experimental conditions for these upward flow experiments that were all conducted in the same column that had been characterized with a longitudinal dispersivity, α_L, through tracer tests. For the emplacement of the 60% IPA (isopropyl alcohol) −40% water solution, the gravity number was at the critical gravity number and the measured dispersivity was that of the tracer, as expected. When this alcohol-water solution was displaced by water, the gravity number (0.69) was much less than the critical gravity number of $M - 1 = 2.6$ and viscously unstable displacement was expected. *Roeder and Falta* [2001] fit a dispersivity of 2 cm to the experimental results as well as utilizing a 3-D simulator to predict the alcohol displacement. The heterogeneity factor in Koval's model was estimated from the tracer dispersivity and the mobility ratio was used in equation (11) to predict the Koval parameter which was then converted into a dispersion coefficient that corresponds to a dispersivity of 1.65 cm that was close to the fitted value of 2 cm. In a second set of experiments utilizing TBA (tert butyl alcohol), the emplacement of the alcohol was predicted to be very stable and the displacement of that alcohol by water was very unstable due to a mobility ratio of 5.7. Koval's model predicts a dispersivity of 2.6 cm compared to Roeder and Falta's fitted dispersivity of 3 cm. The stability criterion and Koval's model provide a first-order estimate of dispersion during vertical miscible displacements that are close to the observations and simpler than the application of UTCHEM to their laboratory column.

8. Summary and Conclusions

[46] Brine transport in porous media has received considerable attention in the literature due to its importance in many applications, but until now there has not been a synthesis of the available data for one-dimensional vertical displacements, either upward or downward. *Hill*'s [1952] approach to displacement front stability adequately describes the conditions for stable displacements when brines migrate vertically downward and are subsequently displaced by freshwater. Dispersion coefficients normalized by tracer dispersion during vertical miscible displacements are extracted from the literature and additional experimental

Table 5. Miscible Displacement Experiments of *Roeder and Falta* [2001] and Comparison With Models

Alcohol	Displacement	ρ_{bot}, g cm^{-3}	ρ_{top}, g cm^{-3}	μ_{bot}, cP	μ_{top}, cP	U, cm s^{-1}	N_G	M	Fitted α_L, cm	Predicted α_L, cm
60% IPA-40% water	alcohol displacing water	0.938	0.998	3.43	0.95	1.32×10^{-3}	−0.72	0.28	0.06	0.06
	water displacing alcohol	0.998	0.938	0.95	3.43	5.0×10^{-3}	0.69	3.6	2	1.65
70% TBA-30% water	alcohol displacing water	0.867	0.998	5.42	0.95	1.92×10^{-3}	−0.69	0.175	0.06	<0.06
	water displacing alcohol	0.998	0.867	0.95	5.42	4.2×10^{-2}	0.18	5.7	3	2.6

determinations are reported that are empirically correlated with the gravity number and the mobility ratio. In region III ($N_G < 0$, $M < 1$) the viscosity contrast contributes little stability for the brines investigated, and Figure 12a provides an estimate of the normalized dispersion coefficient as a function of gravity number. For gravity numbers more negative than −1.0, gravitational instability dominates and a dispersion model becomes questionable. In region I ($N_G > 0$, $M > 1$), gravitational stability reduces dispersion below that of tracers as quantified in Figure 14b for $N_G > N_{G,c}$, and the asymptotic value of the dispersion coefficient at $N_G = 0$ can be estimated from Koval's model.

[47] These empirical results are specific to the conditions encountered at the interface between freshwater and high concentration salt solutions where the density and viscosity both increase with concentration. The results cannot be immediately applied to light, viscous fluids or heavy, low-viscosity fluids such are encountered in the miscible recovery of petroleum products or DNAPLs where the range in mobility ratio can be much greater. Extrapolation of these results and the analysis from the idealized laboratory to the field remains a challenge since field conditions are not one-dimensional, the horizontal extent of the brine source and its release rate are both likely to be significant, and the subsurface is heterogeneous. The continued occurrence of dense brines with associated contaminants and the injection and recovery of fluids miscible with water that are not matched for density or viscosity suggest the necessity of further investigation of brine transport in the subsurface.

Appendix A

[48] This research was fortunate in having published data available where investigators report dispersion coefficients for miscible displacements, mostly with brines, but a few utilized organic solvents. This appendix summarizes the procedures utilized to extract dispersion coefficients from the published data.

A1. *Biggar and Nielsen* [1964]

[49] Concentrations of the resident and the displacing fluids are reported along with column properties. The permeability was estimated from reported values of the porosity and the grain size using the Kozeny-Carmen relationship

$$k = \frac{n^3}{180(1-n)^2} d_g^2 \tag{A1}$$

Tracer dispersion utilized *Biggar and Nielsen*'s [1964] Figure 4 assuming the dispersion coefficient was proportional to pore water velocity. For the viscously unstable displacements in their Figure 5, the dispersion coefficients were estimated by fitting the error function solution to the data:

$$\frac{C}{C_0} = \frac{1}{2}\left[1 - erf\left(\frac{x - U_{Pore}t}{2\sqrt{D_{PM}t}}\right)\right] \tag{A2}$$

where x is the position along the mean flow path and t is time. If the column is assumed to be infinitely long so that the end effects can be neglected, the positions of 5% ($x_{0.05}$) and 95% ($x_{0.95}$) of the displacing fluid when the center of mass has traveled the length of the column are calculated from

$$\begin{aligned} 0.05 &= \frac{1}{2}\left[1 - erf\left(\frac{x_{0.05} - L_{Column}}{2\sqrt{D_{PM}\dfrac{L_{Column}}{U_{Pore}}}}\right)\right] \\ &\Rightarrow \frac{x_{0.05} - L_{Column}}{2\sqrt{D_{PM}\dfrac{L_{Column}}{U_{Pore}}}} \\ &= erf^{-1}(0.9) \\ 0.95 &= \frac{1}{2}\left[1 - erf\left(\frac{x_{0.95} - L_{Column}}{2\sqrt{D_{PM}\dfrac{L_{Column}}{U_{Pore}}}}\right)\right] \\ &\Rightarrow \frac{x_{0.95} - L_{Column}}{2\sqrt{D_{PM}\dfrac{L_{Column}}{U_{Pore}}}} \\ &= erf^{-1}(-0.9) \end{aligned} \tag{A3}$$

where erf^{-1} represents the inverse error function and $erf^{-1}(0.9)$ is approximately 1.163. The length of the transition zone is calculated as

$$L_T = x_{0.05} - x_{0.95} = 4erf^{-1}(0.9)\sqrt{D_{PM}\frac{L_{Column}}{U_{Pore}}} \tag{A4}$$

Rearranging equation (A4) provides an estimate of the dispersion coefficient:

$$D_{PM} = \left(\frac{L_T}{4erf^{-1}(0.9)}\right)^2 \frac{U_{Pore}}{L_{Column}} \tag{A5}$$

A2. *Slobod and Howlett* [1964]

[50] The physical properties of the resident and the displacing fluids are reported. The grain size was estimated

from reported values of the permeability and porosity using the Kozeny-Carmen equation. The mixing behavior is reported as the length of the transition zone, L_T, between the breakthrough of 5% and 95% of the displacing fluid and the dispersion coefficient was determined from the application of equation (A5). Tracer dispersion was estimated using the experimental correlation of Perkins and Johnston (equation (6)). A number of the experiments had no density contrast and these were plotted as having a gravity number of 10^{-3}.

A3. *Elrick et al.* [1966]

[51] All of the relevant column and fluid properties are reported along with dispersion coefficients. Tracer dispersion coefficients are estimated from equation (6).

A4. *Krupp and Elrick* [1969]

[52] The permeability was estimated from reported values of the porosity and the grain diameter using the Kozeny-Carmen relationship. The displacement direction, pore water velocity, and dispersivity for each experimental realization were reported. Tracer dispersion coefficients were estimated using equation (6). Brine dispersion coefficients were read off their Figure 8.

A5. *Starr and Parlange* [1976]

[53] *Starr and Parlange* [1976] reported all relevant column and brine properties. Their Figure 1 demonstrates that tracer dispersion was proportional to velocity. Dispersion coefficients are obtained from fitting the breakthrough curves over the interval $0 < C/C_o < 0.5$ since tailing is observed at longer times. Because of high uncertainty the dispersion coefficient for upward flow at the low velocity for 0.01 N $CaCl_2$ displacing 1.0 N $CaCl_2$ is not included.

A6. *Aachib* [1987]

[54] The displacing fluid was reported to be distilled water, but no specific resident fluid concentrations were reported. Rather, the resident fluids were characterized in terms of a modified Prandtl number

$$\mathrm{Pr}^* = \frac{10^6 D_{mol} \Delta\rho}{\mu_{mean}} \tag{A6}$$

For each resident fluid, concentration was calculated from the reported values of the modified Prandtl number, and the density and viscosity were estimated from published data and a molecular diffusivity of 1.34×10^{-5} cm^2 s^{-1} was assumed for $CaCl_2$. Brine dispersion coefficients normalized by molecular diffusivity are reported for each experiment. Tracer dispersion coefficients were estimated using equation (6).

A7. *Buès and Aachib* [1991]

[55] The porosity was estimated from reported values of the grain size and the permeability using the Kozeny-Carmen relationship. The resident fluid was reported to be distilled water, but no specific displacing fluid concentrations were reported. Rather, the displacing fluids were characterized in terms of a modified Prandtl number as in the work by *Aachib* [1987], and they included a figure relating the modified Prandtl number to the concentration in grams of calcium chloride per liter of solution. Using this figure, the concentration was calculated from the reported values of the modified Prandtl number. The density and viscosity of the resident and the displacing fluids were estimated from published data. The measured dispersivity at various molecular Peclet and modified Prandtl numbers are reported as a function of length along the soil column. Pore water velocity was calculated from the molecular Peclet number and the asymptotic, whole column, value of the dispersion coefficient. Tracer dispersion is estimated using the Perkins and Johnston method (equation (6)).

A8. *Kempers and Haas* [1994]

[56] The sandstone has a reported pore size of 2.8×10^{-5} m, but no value of grain size is estimated for the compilation table. Brine dispersion coefficients are reported for each experimental realization. Tracer dispersivity is estimated from the highest water flow velocity. While gas-oil displacements were reported in the "B" series of experiments, those results are not utilized because it was not possible to determine tracer dispersion.

A9. *Harmon et al.* [1999]

[57] The physical properties of the resident and the displacing fluids are estimated using published data [*Lide*, 2000], and all column properties are reported. Dispersion for viscously stable and the viscously unstable displacements is obtained by fitting the error function solution to the data using the method in equation (A5). Tracer dispersion was estimated using the Perkins and Johnston method (equation (6)).

A10. *Schotting et al.* [1999]

[58] The densities of the resident and the displacing fluids were reported. The permeability of the column is estimated from reported values of the grain size and the average porosity using the Kozeny-Carmen relationship. The dispersivity under tracer conditions was estimated using the Perkins and Johnston method (equation (6)).

A11. *Watson et al.* [2002]

[59] The column and fluid properties are given in the paper and tracer dispersion coefficients were predicted using their Figures 21 and 22 for the coarse and medium sand, respectively, using the linear dependency on seepage velocity passing through the dispersion data at the lowest salt concentration (5 g/L) and the highest velocity (lowest gravity number). Hydrodynamic dispersion coefficients at up to four locations within the column are reported and included in the data compilation.

A12. *Jiao and Hötzl* [2004]

[60] Most of the experiments are for NaCl solutions and they report a Rayleigh Number from which density differences are calculated assuming the other solution was salt-free water. The reported particle Peclet number was $250 = d_p U/D_{mol}$, and assuming $D_{mol} = 1.58 \times 10^{-5}$ cm^2 s^{-1} [*Lide*, 2000] provides an estimate of 0.079 cm s^{-1} for the pore water velocity that was used in the calculation of gravity number. Experimental results were reported in their Figure 11 as the coefficient of hydrodynamic dispersion, α_L, and tracer dispersivity is estimated from the data with a α_L value of 0.50 cm. Six slightly stable experiments were

conducted to investigate the effect of the mobility ratio on the dispersion coefficient using water, glycerol and NaCl solutions. Their Figure 12 plotted the ratio of hydrodynamic dispersion coefficient normalized by the hydrodynamic dispersion coefficient at M = 1 against the mobility ratio. Their Table 2 reported the density difference, the velocity, and the mobility ratio, the dispersion coefficient and the dispersivity. It is worth noting that the M = 1 experimental results arrived at α_L = 0.85 cm compared to the adopted value of 0.50 cm for the dilute NaCl experiments.

A13. *Menand and Woods* [2005]

[61] Unlike the other experiments that were done in columns, these researchers utilized a 1 cm by 15 cm cross section that was 23.5 cm tall to observe and photographically quantify stable and unstable vertical displacements. From the reported density differences, NaCl concentrations and brine viscosity were determined by interpolation from published data. T. Menand (personal communication, 2006) provided numerical data appearing in their Figures 5 and 9 along with correcting their Figure 5 caption. Tracer dispersion in the apparatus was determined from reported data and fitted to the function

$$D_T = 0.29 \times 10^{-5} Pe^{1.13} \quad \text{(A7)}$$

where D_T is in cm^2 s^{-1} and the particle Peclet number is $Pe = v_s a/D_o$ with v_s as the reported Darcy velocity, a is the glass bead diameter, and D_o is an assumed molecular diffusivity of NaCl. Apparatus dispersion coefficients under stable displacements were read off their Figure 5 and those that appeared diffusive under unstable conditions were obtained from *Menand and Woods'* [2005] Figure 9. Experimental results for their unstable gravity numbers greater than about 1.5 were not dispersive and the authors did not report dispersion coefficients.

A14. Other Data

[62] Not all previously published vertical miscible displacement data are included in this synthesis. *Bachmat and Elrick* [1970] investigate density-driven instabilities in a one-dimensional soil column that was closed at the bottom. Fluid from a brine-filled reservoir attached to the top of the column would penetrate into the sand pack. The degree of penetration of the dense fluid into the column was quantified by measuring the decrease of salt concentration in the reservoir as a function of time. However, as the salt concentration decreased, the driving force for density-driven flow also decreased. These inconsistencies in the upper boundary condition limited the use of this data set. The experiments of *LaFolie et al.* [1997] are conducted in a small column (length = 3.4 cm, diameter = 2.35 cm) with a large grain size (diameter = 4 to 5 mm). This column represented a porous medium with only five to six grains in the direction of the displacement and seven to eight grains in the plane perpendicular to the direction of the displacement. Since their apparatus was small compared to the grain size, it was not representative of a large-scale porous medium and their data are not included. *Wood et al.* [2004] applied a 0.05 pore volume pulse of dense fluid and breakthrough curves are shown and dispersivities are reported. A constant head driving force resulted in a variable flow rate, and the short-duration pulse does not correspond to the step input function needed for the analysis of displacement processes. In addition, the authors questioned the applicability of the advection-dispersion model for this system.

[63] **Acknowledgments.** This work was supported by the National Institute of Environmental Health Sciences Superfund Basic Research Program at University of California Berkeley (NIH P42 ES04705), the University of California Water Resources Center, and the American Geophysical Union Horton Research Grant. The authors are grateful to Claire Welty for providing access to Aachib's thesis, Thierry Menand for sending a tabulation of his published data, and Associate Editor John Selker and three reviewers for their thoughtful comments.

References

Aachib, M. (1987), Displacement Isotherme de Deux Fluides Miscibles dans un Milieu Poreux Sature: Effets de Densite et de Viscosite, Critere de Stabilite, Doctoral thesis, Univ. Louis Pasteur, Strasbourg, France.

American Water Works Association (AWWA) (1990), *Water Quality and Treatment, A Handbook of Community Water Supplies*, 4th ed., McGraw Hill, New York.

Aratani, T., K. Yahikozawa, H. Matoba, S. Yasuhara, and T. Yano (1978a), Conditions for the precipitation of heavy metals from wastewater by the lime sulfurated solution (calcium polysulfide) process, *Bull. Chem. Soc. Jpn.*, *51*(6), 1755–1760.

Aratani, T., Y. Nakata, H. Matoba, S. Yasuhara, and T. Yano (1978b), The removal of heavy metal, phosphate, and COD substances from wastewater by the lime sulfurated solution (calcium polysulfide) process, *Bull. Chem. Soc. Jpn.*, *51*(9), 2705–2709.

Bachmat, Y., and D. E. Elrick (1970), Hydrodynamic instability of miscible fluids in a vertical porous column, *Water Resour. Res.*, *6*, 156–171.

Barth, G. R., T. H. Illangasekare, M. C. Hill, and H. Rajaram (2001), A new tracer-density criterion for heterogeneous porous media, *Water Resour. Res.*, *37*(1), 21–31.

Bell, J. T., and L. H. Bell (1994), Separations technology: The key to radioactive waste minimization, in *Chemical Pretreatment of Nuclear Waste for Disposal*, edited by W. W. Schulz and E. P. Horwitz, pp. 1–35, Springer, New York.

Biggar, J. W., and D. R. Nielsen (1964), Chloride-36 diffusion during stable and unstable flow through glass beads, *Soil Sci. Soc. Am. Proc.*, *28*, 591–595.

Buckley, S. E., and M. C. Leverett (1942), Mechanism of fluid displacement in sands, *Trans. Am. Inst. Min. Metall. Eng.*, *146*, 107–116.

Buès, M. A., and M. Aachib (1991), Influence of the heterogeneity of the solutions on the parameters of miscible displacement in saturated porous-medium. 1. Stable displacement with density and viscosity contrasts, *Exp. Fluids*, *11*, 25–32.

Diersch, H.-J. G., and O. Kolitz (2002), Variable density flow and transport in porous media: Approaches and challenges, *Adv. Water Resour.*, *25*, 899–944.

Durmusoglu, E., and M. Y. Corapcioglu (2000), Experimental study of horizontal barrier formation by colloidal silica, *J. Environ. Eng.*, *126*, 833–841.

Elrick, D. E., K. T. Erh, and H. K. Krupp (1966), Applications of miscible displacement techniques to soils, *Water Resour. Res.*, *2*(4), 717–727.

Flowers, T. C. (2003), Brine transport in the subsurface: Analysis of mechanisms and implications for groundwater contamination, Ph.D. thesis, Univ. of Calif., Berkeley.

Flowers, T. C., and J. R. Hunt (2000), Long term release of perchlorate as a potential source of groundwater contamination, in *Perchlorate in the Environment*, edited by E. T. Urbansky, pp. 177–188, Springer, New York.

Freeze, R. A., and J. A. Cherry (1979), *Groundwater*, Prentice Hall, Upper Saddle River, N. J.

Fried, J. J., and M. A. Combarnous (1971), Dispersion in porous media, *Adv. Hydrosci.*, *7*, 169–282.

Frind, E. O. (1982), Simulation of long-term transient density-dependent transport in groundwater, *Adv. Water Resour.*, *5*, 73–88.

Gettinby, J. H., R. W. Sarsby, and J. Nedwell (1996), The composition of leachate from landfilled refuse, *Proc. Inst. Civ. Eng. Municip. Eng.*, *115*, 47–59.

Gibbons, R. D., D. G. Dolan, H. May, K. O'Leary, and R. O'Hara (1999), Statistical comparison of leachate from hazardous, codisposal, and municipal solid waste landfills, *Ground Water Monit. Remed.*, *19*(4), 57–72.

Grubb, D. G., and N. Sitar (1999), Horizontal ethanol floods in clean, uniform, and layered sand packs under confined conditions, *Water Resour. Res.*, *35*(11), 3291–3302.

Harmon, T. C., T. J. Kim, B. K. Dela Barre, and C. V. Chrysikopoulos (1999), Cosolvent-water displacement in one-dimensional soil column, *J. Environ. Eng.*, *125*(1), 87–91.

Hassanizadeh, S. M., and T. Leijnse (1988), On the modeling of brine transport in porous-media, *Water Resour. Res.*, *24*(3), 321–330.

Hassanizadeh, S. M., and A. Leijnse (1995), A non-linear theory of high-concentration-gradient dispersion in porous media, *Adv. Water Resour.*, *18*(4), 203–215.

Herbert, A. W., C. P. Jackson, and D. A. Lever (1988), Coupled groundwater flow and solute transport with fluid density strongly dependent upon concentration, *Water Resour. Res.*, *24*(10), 1781–1795.

Hill, S. (1952), Channeling in packed columns, *Chem. Eng. Sci.*, *1*(6), 247–253.

Homsy, G. M. (1987), Viscous fingering in porous-media, *Annu. Rev. Fluid Mech.*, *19*, 271–311.

Istok, J. D., and M. D. Humphrey (1995), Laboratory investigation of buoyancy-induced flow (plume sinking) during 2-well tracer tests, *Ground Water*, *33*(4), 597–604.

Jacobs, J., R. L. Hardison, and J. V. Rose (2001), In-situ remediation of heavy metals using sulfur-based treatment technologies, *Hydrovisions*, *10*(2), 1, 4, 5.

Jiao, C.-Y., and H. Hötzl (2004), An experimental study of miscible displacements in porous media with variation of fluid density and viscosity, *Transp. Porous Media*, *54*, 125–144.

Johnson, D. N., J. A. Pedit, and C. T. Miller (2004), Efficient, near-complete removal of DNAPL from three-dimensional, heterogeneous porous media using a novel combination of treatment technologies, *Environ. Sci. Technol.*, *38*(19), 5149–5156.

Kempers, L. J. T. M., and H. Haas (1994), The dispersion zone between fluids with different density and viscosity in a heterogeneous porous-medium, *J. Fluid Mech.*, *267*, 299–324.

Kolditz, O., R. Ratke, H.-J. G. Diersch, and W. Zielke (1998), Coupled groundwater flow and transport: 1. Verification of variable density flow and transport models, *Adv. Water Resour.*, *21*(1), 27–46.

Koval, E. J. (1963), A method for predicting the performance of unstable miscible displacement in heterogeneous media, *Trans. Soc. Petrol. Eng. AIME*, *228*, 145–154.

Krupp, H. K., and D. E. Elrick (1969), Density effects in miscible displacement experiments, *Soil Sci.*, *107*(5), 372–380.

LaFolie, F., C. Hayot, and D. Schweich (1997), Experiments on solute transport in aggregated porous media: Are diffusions within aggregates and hydrodynamic dispersion independent?, *Transp. Porous Media*, *29*, 281–307.

Lake, L. W. (1989), *Enhanced Oil Recovery*, Prentice-Hall, Upper Saddle River, N. J.

Lapwood, E. R. (1948), Convection of a fluid in a porous medium, *Proc. Cambridge Philos. Soc.*, *44*, 508–521.

Lide, D. R. (2000), *CRC Handbook of Chemistry and Physics*, 81st ed., CRC Press, Boca Raton, Fla.

List, E. J. (1965), The stability and mixing of a density stratified horizontal flow in a saturated porous medium, *Rep. KH-R-11*, Calif. Inst. of Technol., Pasadena.

Liu, H. H., and J. H. Dane (1997), A numerical study on gravitational instabilities of dense aqueous phase plumes in three-dimensional porous media, *J. Hydrol.*, *194*, 126–142.

Manickam, O., and G. M. Homsy (1995), Finger instabilities in vertical miscible displacement flows in porous media, *J. Fluid Mech.*, *288*, 75–102.

Mazzia, A. A., L. Bergamaschi, and M. Putti (2001), On the reliability of numerical solutions of brine transport in groundwater: Analysis of infiltration from a salt lake, *Transp. Porous Media*, *43*(1), 65–86.

Menand, T., and A. W. Woods (2005), Dispersion, scale, and time dependence of mixing zones under gravitationally stable and unstable displacements in porous media, *Water Resour. Res.*, *41*, W05014, doi:10.1029/2004WR003701.

Nelson, M. D., B. L. Parker, T. A. Al, J. A. Cherry, and D. Loomer (2001), Geochemical reactions resulting from in-situ oxidation of PCE-DNAPL by $KMnO_4$ in a sandy aquifer, *Environ. Sci. Technol.*, *35*, 1266–1275.

Nordstrom, D. K., C. N. Alpers, C. J. Ptacek, and D. W. Blowes (2000), Negative pH and extremely acidic mine waters from Iron Mountain, California, *Environ. Sci. Technol.*, *34*, 254–258.

Oldenburg, C. M., and K. Pruess (1998), Layered thermohaline convection in hypersaline geothermal systems, *Transp. Porous Media*, *33*, 29–63.

Oliviera, I. B., A. H. Demond, and A. Salehzadeh (1996), Packing of sands for the production of homogeneous porous media, *Soil Sci. Soc. Am. J.*, *60*, 49–53.

Oostrom, M., J. S. Hayworth, J. H. Dane, and O. Güven (1992), Behavior of dense aqueous phase leachate plumes in homogeneous porous media, *Water Resour. Res.*, *28*(8), 2123–2134.

Oswald, S. E., and W. Kinzelbach (2004), Three-dimensional physical benchmark experiments to test variable-density flow models, *J. Hydrol.*, *290*, 22–42.

Perkins, T. K., and O. C. Johnston (1963), A review of diffusion and dispersion in porous media, *Trans. Soc. Petrol. Eng. AIME*, *228*, 70–84.

Riaz, A., and E. Meiburg (2003), Three-dimensional miscible displacement simulations in homogeneous porous media with gravity override, *J. Fluid Mech.*, *494*, 95–117.

Roeder, E., and R. W. Falta (2001), Modeling unstable alcohol flooding of DNAPL-contaminated columns, *Adv. Water Resour.*, *24*, 803–819.

Saffman, P. G., and G. Taylor (1958), The penetration of a fluid into a porous medium or Hele-Shaw cell containing a more viscous liquid, *Proc. R. Soc. London, Ser. A*, *245*, 312–329.

Samsonova, L. M., and E. Drozhko (1996), Migration of high-density industrial waste solutions through fresh groundwaters, in *Deep Injection Disposal of Hazardous and Industrial Waste: Scientific and Engineering Aspects*, edited by J. A. Apps and C. F. Tsang, pp. 669–680, Elsevier, New York.

Schincariol, R. A. (1998), Dispersive mixing dynamics of dense miscible plumes: Natural perturbation initiation by local-scale heterogeneities, *J. Contam. Hydrol.*, *34*(3), 247–271.

Schincariol, R. A., and F. W. Schwartz (1990), An experimental investigation of variable density flow and mixing in homogeneous and heterogeneous media, *Water Resour. Res.*, *26*(6), 2317–2319.

Schincariol, R. A., F. W. Schwartz, and C. A. Mendoza (1994), On the generation of instabilities in variable density flow, *Water Resour. Res.*, *30*(4), 913–927.

Schotting, R. J., H. Moser, and S. M. Hassanizadeh (1999), High-concentration-gradient dispersion in porous media: Experiments, analysis and approximations, *Adv. Water Resour.*, *22*(7), 665–680.

Schumacher, J. G. (1960), *Perchlorates: Their Properties, Manufacture, and Uses*, Reinhold, New York.

Simmons, C. T., K. A. Narayan, and R. A. Wooding (1999), On a test case for density-dependent groundwater flow and solute transport models: The salt lake problem, *Water Resour. Res.*, *35*(12), 3607–3620.

Simmons, C. T., T. R. Fenstemaker, and J. M. Sharp, Jr. (2001), Variable-density groundwater flow and solute transport in heterogeneous porous media: Approaches, resolutions, and future challenges, *J. Contam. Hydrol.*, *52*, 245–275.

Simmons, C. T., M. L. Pierini, and J. L. Hutson (2002), Laboratory investigation of variable-density flow and solute transport in unsaturated-saturated porous media, *Transp. Porous Media*, *47*, 215–244.

Slobod, R. L., and W. E. Howlett (1964), The effects of gravity segregation in laboratory studies of miscible displacement in vertical unconsolidated porous media, *Trans. Soc. Petrol. Eng. AIME*, *231*, 1–8.

Song, D. L., M. E. Conrad, K. S. Sorenson, and L. Alvarez-Cohen (2002), Stable carbon isotope fractionation during enhanced in situ bioremediation of trichloroethylene, *Environ. Sci. Technol.*, *36*(10), 2262–2268.

Sorbie, K. S., H. R. Zhang, and N. B. Tsibuklis (1995), Linear viscous fingering: New experimental results, direct simulation and the evaluation of averaged models, *Chem. Eng. Sci.*, *50*, 601–606.

Stalkup, F. I. (1983), *Miscible Displacement*, Soc. of Pet. Eng. of AIME, Dallas, Tex.

Starr, J. L., and J. Y. Parlange (1976), Solute-dispersion in saturated soil columns, *Soil Sci.*, *121*(6), 364–372.

Swartz, C. H., and F. W. Schwartz (1998), An experimental study of mixing and instability development in variable-density systems, *J. Contam. Hydrol.*, *34*, 169–189.

Toride, N., F. Leij, and M. T. van Genuchten (1999), The CXTFIT code for estimating transport parameters from laboratory or field tracer experiments, *Res. Rep. 137*, U.S. Salinity Lab., Riverside, Calif.

U.S. Environmental Protection Agency (2000), Toxics criteria for states those states not complying with Clean Water Act section 303(c)(2)(B), 40 CFR Ch. I, section 131.36, http://www.epa.gov/ost/standards/wqslibrary/ak/131.36.pdf (accessed 24 October 2005).

Watson, S. J., D. A. Barry, R. J. Schotting, and S. M. Hassanizadeh (2002), Validation of classical density-dependent solute transport theory for stable, high-concentration-gradient brine displacements in coarse and medium sands, *Adv. Water Resour.*, *25*, 611–635.

Welty, C., and L. W. Gelhar (1991), Stochastic analysis of the effects of fluid density and viscosity variability on macrodispersion in heterogeneous porous media, *Water Resour. Res.*, *27*(8), 2061–2075.

Welty, C., and L. W. Gelhar (1992), Simulation of large-scale transport of variable density and viscosity fluids using a stochastic mean model, *Water Resour. Res.*, *28*(3), 815–827.

Wood, M., C. T. Simmons, and J. L. Hutson (2004), A breakthrough curve analysis of unstable density-driven flow and transport in homogeneous porous media, *Water Resour. Res.*, *40*, W03505, doi:10.1029/2003WR002668.

Wooding, R. A. (1959), The stability of a viscous liquid in a vertical tube containing porous material, *Proc. R. Soc. London Ser. A, Math. Phys. Sci.*, *252*, 120–134.

Xu, J., Y. Song, B. Min, L. Steinberg, and B. E. Logan (2003), Microbial degradation of perchlorate: Principles and applications, *Environ. Eng. Sci.*, *20*(5), 405–422.

Yahikozawa, K., T. Aratani, R. Ito, T. Sudo, and T. Yano (1978), Kinetic studies on the lime sulfurated solution (calcium polysulfide) process for removal of heavy metals from wastewater, *Bull. Chem. Soc. Jpn.*, *51*(2), 613–617.

Zhang, H. B., and F. W. Schwartz (1995), Multispecies contaminant plumes in variable-density flow systems, *Water Resour. Res.*, *31*(4), 837–847.

T. C. Flowers, Exponent Inc., 149 Commonwealth Drive, Menlo Park, CA 94025, USA.

J. R. Hunt, Department of Civil and Environmental Engineering, University of California, 760 Davis Hall, Berkeley, CA 94720-1710, USA. (hunt@ce.berkeley.edu)